

## REPORT 1087

### INTERNAL-LIQUID-FILM-COOLING EXPERIMENTS WITH AIR-STREAM TEMPERATURES TO 2000° F IN 2- AND 4-INCH-DIAMETER HORIZONTAL TUBES<sup>1</sup>

By GEORGE R. KINNEY, ANDREW E. ABRAMSON, and JOHN L. SLOOP

#### SUMMARY

*An investigation was conducted to determine the effectiveness of liquid-cooling films on the inner surfaces of tubes containing flowing hot air. Experiments were made in 2- and 4-inch-diameter straight metal tubes with air flows at temperatures from 600° to 2000° F and diameter Reynolds numbers from 2.2 to  $14 \times 10^4$ . The film coolant, water, was injected around the circumference at a single axial position on the tubes at flow rates from 0.02 to 0.24 pound per second per foot of tube circumference (0.8 to 12 percent of the air flow).*

*Visual observations of liquid-film flows were made in transparent tubes at flow conditions similar to those of the film-cooling experiments. The visual experiments were conducted with air flows at temperatures of 80° and 800° F and diameter Reynolds numbers from 4.1 to  $29 \times 10^4$ . Flows of water, water-detergent solutions, and aqueous ethylene glycol solutions (which varied viscosity and surface tension) were investigated.*

*Liquid-coolant films were established and maintained around and along the tube wall in cocurrent flow with the hot air. The tube wall was kept below the boiling temperature of the coolant over the surfaces covered by liquid coolant; little additional cooling of the tube was obtained downstream of the point at which all liquid was vaporized. Coolant films were relatively smooth unless the coolant flow was sufficiently high so that the liquid film was thick enough to enter the region where turbulent forces predominate over viscous forces; wavelike disturbances then developed on the liquid film. These disturbances resulted in increased loss of coolant from the film and reduced effectiveness of the coolant. Predictions could be made of the approximate highest coolant flow which could be introduced at a single axial position in the tubes to form a liquid film without the effectiveness of the coolant being reduced by the formation of disturbances. The results indicated that, in order to film cool a given surface area with as little coolant flow as possible, it may be necessary to limit the flow of coolant introduced at any single axial position and to introduce it at several axial positions.*

*The flow rate of inert coolant required to maintain liquid-film cooling over a given area of tube surface can be estimated when the gas-flow conditions are known by means of a generalized plot of the film-cooling data.*

#### INTRODUCTION

Combustion chambers and ducts which are subjected to extremely high heat transfer from flowing hot gases may be difficult to cool by the conventional method of circulating

a fluid over the outer surfaces of the walls. Other methods of cooling may be used as, for example, sweat cooling, where the duct wall is made of a porous material and the cooling fluid is forced through the wall in the opposite direction to the heat flow. Another approach is to give the inner surface of the duct some form of protection, which prevents most of the heat from reaching it. This protection may be in the form of a coating or liner of a high-temperature-resistant insulator, or the surface may be covered with a layer of cooling fluid which absorbs the heat (internal-film cooling).

Investigations of sweat cooling with gases flowing through porous walls are reported in references 1 to 6, in which theoretical and experimental data indicate the amount of gaseous coolant required to maintain a porous wall at a given temperature for known gas-stream conditions. The use of sweat cooling in applications where the coolant flow must be well controlled and must vary throughout the walls to be cooled (such as in a rocket engine) has been limited because of difficulty in fabricating porous walls to meet the requirements.

The use of high-temperature-resisting materials to reduce the heat flow into rocket-engine walls is described in references 1 and 7. This method has been used successfully with rocket engines operating for short durations without cooling and on other rocket engines to reduce the amount of external cooling required.

Large reductions in over-all heat transfer to rocket-engine walls have been obtained by internal-film cooling with the use of relatively small quantities of liquid coolant (references 8 and 9). Investigations concerned with establishing liquid-cooling films for rocket engines are described in references 1 and 10. Liquids are more effective than gases as internal-film coolants because of their higher heat-absorption capacity (including heat of vaporization) and because less turbulent mixing of the coolant with the hot gas stream occurs with a liquid film than with a gas.

A schematic representation of a liquid-cooling film vaporizing in an air stream is shown in figure 1. Heat is transferred from the hot air stream to the coolant film, and, simultaneously, mass transfer from the coolant to the air occurs as the coolant vaporizes. Experimental investigation of the simultaneous transfer of heat and mass has been limited to gas-stream temperatures and Reynolds numbers much lower than anticipated for film-cooling applications. Reference 11 gives the results of such experiments with low

<sup>1</sup>Supersedes NACA RM E50F19, "Internal Film Cooling Experiments in 4-Inch Duct with Gas Temperatures to 2000° F" by George R. Kinney and John L. Sloop, 1950; NACA RM E51C13, "Investigation of Annular Liquid Flow with Cocurrent Air Flow in Horizontal Tubes" by George R. Kinney and Andrew E. Abramson, 1951; NACA RM E52B20, "Internal-Film-Cooling Experiments with 2- and 4-Inch Smooth-Surface Tubes and Gas Temperatures to 2000° F" by George R. Kinney, 1952.



calming chamber 12 inches in diameter. Test sections of 2- and 4-inch diameter were used. They consisted of an Inconel approach section 40 inches long, a coolant injector, and a film-cooled or transparent tube 48 inches long. The exhaust section contained a series of water sprays to quench hot air; this section was connected to the laboratory exhaust system. An expansion bellows installed downstream of the exhaust-quenching sprays allowed for expansion of the apparatus when the 4-inch-diameter film-cooled tubes were used; the 2-inch-diameter film-cooled tube and the transparent tubes fitted into packed housings to allow for expansion of the apparatus.

#### COOLANT-INJECTION SYSTEM

The coolant-injection system consisted of a supply reservoir, filters, a positive-displacement pump, adjustable pressure regulators (which controlled flow), rotameters, and coolant injectors.

For most of the film-cooling experiments and all the visual-flow experiments, porous-surface coolant injectors (fig. 3(a)) were used. There were two such injectors of similar construction, one for the 2-inch and one for the 4-inch test section. They consisted of a metal ring with slots milled into the inner surface about the circumference. The 2- and 4-inch-diameter coolant injectors had 60 and 90 slots, respectively. Holes 0.013 inch in diameter were drilled through the ring into each of the slots. A housing, which provided a supply annulus for the coolant, fitted over the ring. The small holes metered the flow into each slot, thus providing a uniform distribution of the flow about the circumference. The slots and the porous-cloth liner spread the coolant flow over a large area at a low velocity. As the liner was very porous (36 mesh), it did not restrict the flow but provided a surface onto which the coolant flowed. The air flow over the surface of the injector carried the coolant downstream along the inner surfaces of the tubes.

The remainder of the heat-transfer experiments were conducted with the jet-type coolant injector shown in figure 3(b). It consisted of a brass ring through which 60 holes were drilled 0.013 inch in diameter equally spaced around the circumference at an angle of 45° to the axis of the ring. A stainless-steel splash ring was fitted into the brass ring; a housing, which provided a supply annulus for the coolant, fitted over the brass ring. The splash ring directed the flow of the coolant downstream and against the surface of the duct; its spacing did not control the coolant flow. The splash ring blocked 5 percent of the gas-flow area.

#### FILM-COOLED TUBES

The heat-transfer experiments were conducted with three different Inconel tubes; each had a  $\frac{1}{8}$ -inch wall and was 48 inches long. Two of them were seamless tubes with honed inner surfaces and are designated as smooth-surface tubes; one had a 2-inch and the other a 4-inch inside diameter. The third, designated as the rough-surface tube, was a 4-inch-inside-diameter rolled tube with a longitudinal weld. Although the inside surface of this tube was machined after welding, some surface roughness and waviness remained. The inner surface of the rough-surface tube was also inter-

rupted by three projecting pressure probes spaced along the length of the tube and 12 holes used for measuring static pressures. The heat loss from the tubes was too small to affect the heat-transfer results.

The visual experiments were conducted with a 4-inch pyrex tube and a 4-inch- and a 2-inch-diameter plastic tube (methyl methacrylate). All tubes were 48 inches long and  $\frac{1}{4}$  inch thick and were sealed to an aluminum adapter by means of a flange; the adapter was sealed to the liquid injector. The other end of the tubes fitted into expansion slip joints.

#### FILM COOLANTS

Water was used as the film coolant for all the heat-transfer experiments. For the visual experiments, a detergent was used to change the surface tension, and ethylene glycol, to change the viscosity. Table I lists some properties of the liquids used. The pressure in the test section varied for the different conditions of the heat-transfer experiments, which resulted in a variation in the boiling temperature of the water of approximately 20° F; the average boiling temperature was 240° F.

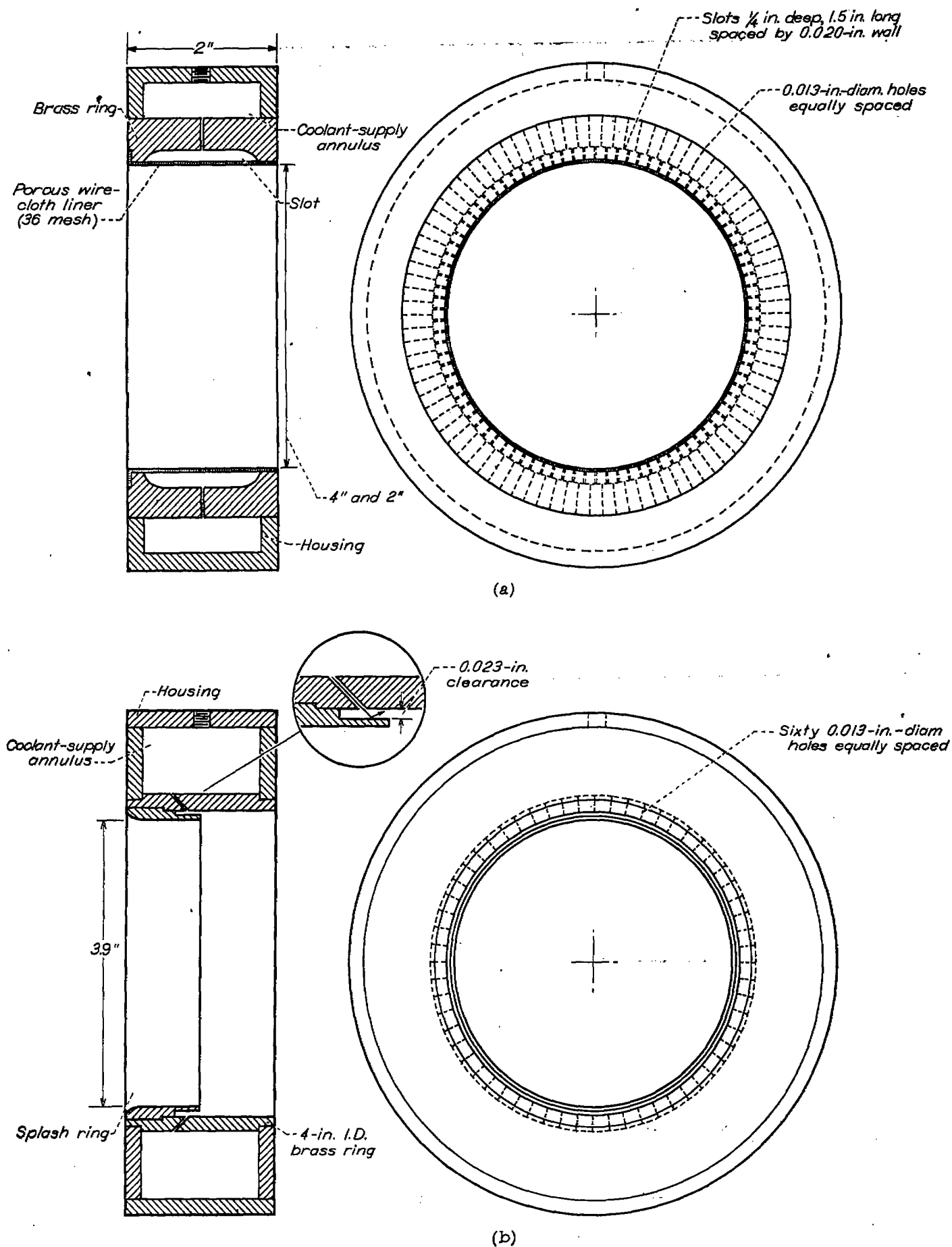
#### INSTRUMENTATION

**Flow rate.**—Air flows were measured within 2 percent by means of orifices and a differential water manometer. Coolant flows were measured within 1 to 4 percent by means of rotameters.

**Pressure.**—The static pressure of the air stream was measured during the heat-transfer experiments in the approach section 3 inches upstream of the coolant injector by means of a mercury manometer. The measurements were used to determine approximate air densities and velocities at this position and to approximate the boiling temperature of the coolant in the film-cooled tube.

**Temperature.**—Air temperatures were measured by means of chromel-alumel thermocouples and a self-balancing potentiometer. Rakes containing 20 thermocouples were located in the calming section and a rake with four thermocouples for the 4-inch test section, and with one thermocouple for the 2-inch test section, was placed in the approach section 3 inches upstream of the coolant injector. The estimated accuracy of air-temperature measurements varied from  $\pm 10^\circ$  at 80° F to  $\pm 25^\circ$  at 2000° F. These values were determined from a consideration of instrument accuracy, wire calibration, radiation and conduction heat losses, and fluctuations of the air-stream temperature during runs. The recovery factor for the thermocouples located in the approach section (where the Mach numbers were from 0.5 to 0.7) was of the order of 0.9; this recovery factor was obtained from a comparison of the thermocouple readings in the approach section with those in the calming section (where Mach numbers were below 0.1). Because the recovery factor was high, the total temperatures as measured by thermocouples in the approach section were used; the differences between the temperatures used and the temperatures obtained by correcting on the basis of recovery factor were less than 1 percent.

Wall temperatures on the Inconel tubes were measured by means of chromel-alumel thermocouples and a recording potentiometer. The thermocouples, which were welded to the outer surface of the tubes, were spaced along the length



(a) Porous surface (used for both heat-transfer and visual experiments).  
 (b) Jet type (used only for heat-transfer experiments).

FIGURE 8.—Coolant injectors

of the tubes at eight positions around the circumference of the 4-inch tubes (table II) and four positions around the circumference of the 2-inch tube (table III). Wall temperatures were measured by these thermocouples within  $\pm 10^\circ\text{F}$ . Liquid temperature was measured within  $\pm 5^\circ\text{F}$  by means of a thermocouple in the supply annulus of the injector.

**Liquid-flow disturbance.**—A stroboscopic light was placed on one side facing the transparent tube and observations of the liquid film were made looking into the tube from the opposite side. The timing of the stroboscopic light was adjusted for optimum visual clarity of disturbances on the liquid film.

Shadowgraph pictures of the liquid film were obtained with the aid of a microflash light source on one side of the transparent tube, suitable condensing lenses, and a camera on the opposite side of the tube. The camera was focused on the liquid-film surface nearer to it. High-speed motion pictures of the liquid flow were obtained using floodlamps on one side of the transparent tube and a high-speed camera on the opposite side. The high-speed camera reached a speed of 2000 frames per second and a timing mark was imposed on the film at 1/1000-second intervals.

#### PROCEDURE

The operating procedure consisted in setting the coolant flow, the air flow, and the air temperature at desired values; allowing a few minutes for conditions to stabilize; and recording the data. The air-flow rate was controlled by a throttling valve in the supply line ahead of the surge tank (fig. 2). The exhaust pressure was maintained nearly constant; therefore, the pressure in the test section varied with the air flow and the temperature. The operating conditions covered the following ranges:

Operating conditions	Heat-transfer experiments	Visual experiments
Air temperature*, °F.....	800-2000	80, 800
Static pressure*, in. Hg abs.....	42-74	
Air flow, lb/sec.....	0.9-7.1	0.7-9.4
Coolant flow, lb/sec.....	0.01-0.22	0.01-0.28
Coolant-flow rate/air-flow rate, percent.....	0.80-12	0.3-21
Coolant flow/circumferential length, lb/sec-ft.....	0.02-0.24	0.027-0.270

\* In the approach section 3 in. upstream of the coolant injector.

These conditions give the following values for the air stream in the approach section 3 inches upstream of the coolant injector:

	Heat-transfer experiments	Visual experiments
Reynolds number.....	$2.2-14.0 \times 10^5$	$4.1-29.0 \times 10^4$
Mach number.....	0.5-0.7	
Air mass velocity, lb/(sec) (sq ft).....	39.4-81.7	30.5-108
Air velocity, ft/sec.....	1000-1700	

Values of specific heat for air were obtained from reference 15 and values of thermal conductivity and viscosity for air were obtained from reference 16. Experimental values of Prandtl number and Schmidt number vary only slightly for the temperature range.

In the visual experiments, the nature of the liquid-film

surface, which changed from relatively smooth to wavelike in appearance with increasing liquid flow, was observed over the range of conditions independently by two observers by means of a stroboscopic light. The agreement between observers on liquid flows for the transition from smooth to disturbed surface was within 10 percent and an average of their results was used. As a check on visual observations, shadowgraph and high-speed motion pictures were taken of the liquid film for various flow conditions.

#### RESULTS OF HEAT-TRANSFER EXPERIMENTS

##### LIQUID-COOLED LENGTH

Cooling effectiveness was determined by plotting the wall temperatures of the film-cooled tube as a function of distance from the point of coolant injection. A typical plot, from a run with the 4-inch tube, is shown in figure 4. The tube-wall temperature remains below the boiling temperature of the coolant (water) for about 19 inches downstream of coolant injection, rises to the boiling temperature, and then rises rapidly, approaching a value near the stagnation temperature of the air-coolant vapor mixture. The liquid-cooled length  $L$  (fig. 4) is determined from an average of the distances for which the wall remained below the boiling temperature of the coolant at the eight circumferential positions. Similar plots were obtained for the 2-inch tube, and the liquid-cooled length was determined from an average of four circumferential positions. For the 4-inch tubes, the agreement of the liquid-cooled length for the eight circumferential positions was within 10 to 15 percent; at very low coolant flows greater variation occurred. For the 2-inch tube, even distribution of the coolant was more difficult to achieve; agreement of liquid-cooled length for the different positions was generally within 25 percent, but in many cases one of the four positions would differ from the others by as much as 40 percent.

The effect of gravity, which tends to decrease the proportionate film thickness in the upper portions of the horizontal tube, resulting in shorter liquid-cooled lengths there, was observable in the data of the 2-inch tube but not in the 4-inch tubes. In the 2-inch tube, liquid-cooled lengths in the upper portion were from 5 to 20 percent shorter than those in the lower portion. No trends in the magnitude of the gravity effect were noticeable with the different air and coolant flows investigated. Gravity effects were not of sufficient magnitude in any of the tubes to affect the trends observed in film cooling.

**Carbon deposition on film-cooled tube.**—Each time a run was made, carbon was deposited around the tube immediately downstream of where liquid coolant ceased for a distance of about  $\frac{1}{2}$  inch. Carbon did not form on the surface covered by the liquid film nor farther downstream where the surface became hotter. These deposits disrupt a liquid film and thereby reduce cooling effectiveness; the rate of carbon deposition and the resulting effect were considerably greater in the 2-inch tube than in the 4-inch tubes. For this reason all the experiments in the 2-inch tube were made so that the liquid-cooled length for each succeeding run was less than on the previous run. After each running period, it was

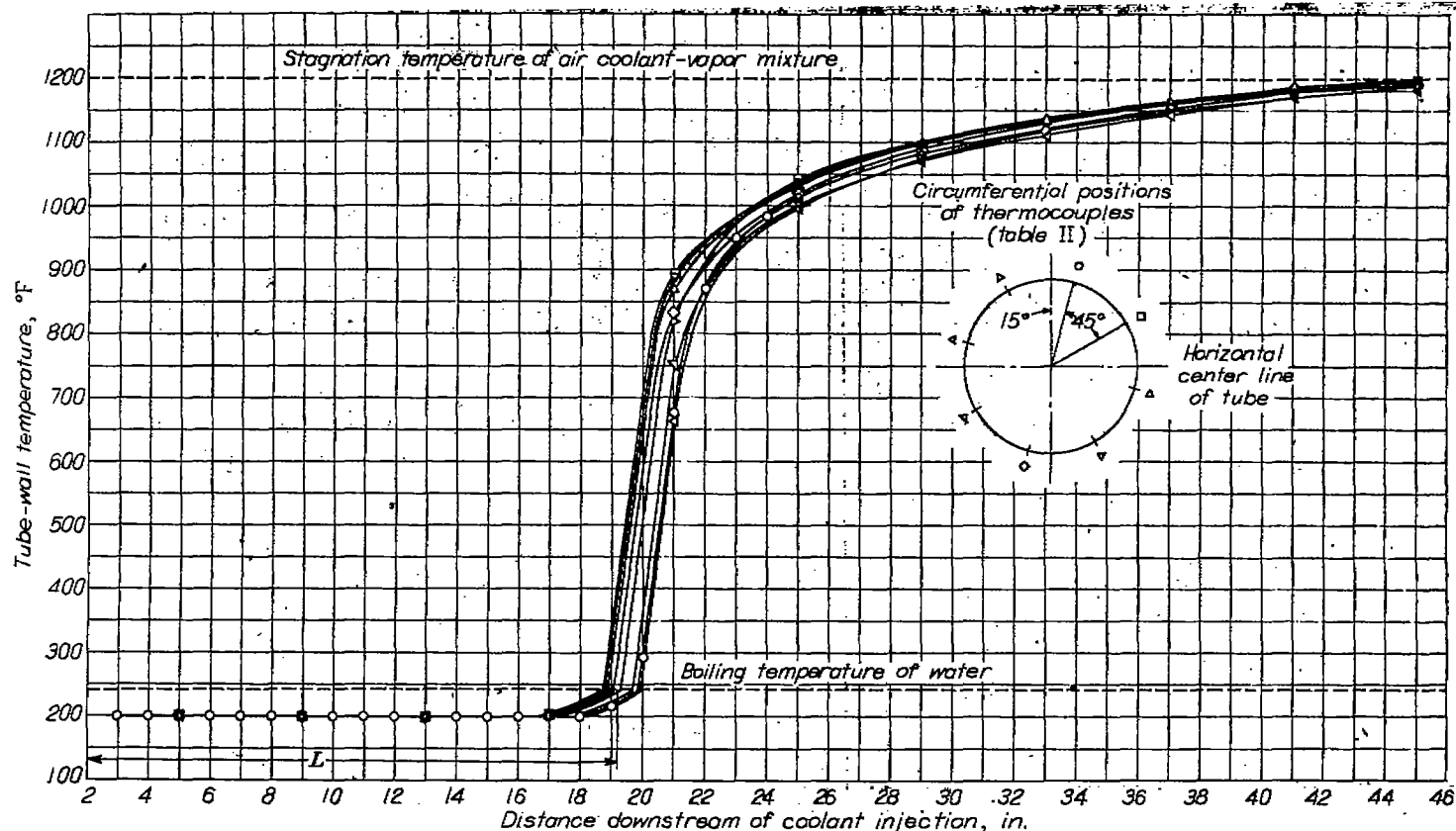


FIGURE 4.—Typical data plot showing liquid-film-cooled length. Smooth-surface tube of 4-inch diameter; air-stream Reynolds number,  $5.3 \times 10^4$ ; air temperature,  $1400^\circ \text{F}$ ; water flow, 0.10 pound per second or 2.6 percent of air flow.

necessary to remove and clean the tube of carbon deposits before further running at long liquid-cooled lengths could be made. Most of the experiments in the 4-inch tubes were also made by means of this procedure; for the other experiments the carbon deposition was not great enough to reduce liquid-cooled lengths more than a few percent.

**Reproducibility of results.**—Consideration of 12 different runs with the 4-inch smooth-surface tube showed that reproducibility of liquid-cooled length at the same experimental conditions was within 5 percent; reproducibility with the 2-inch smooth-surface tube was within 5 percent for six runs, but variations of 15 percent were obtained with three others. The reason for the large variations with some of the runs with the 2-inch tube was attributed to small changes in alinement between coolant injector and tube when the apparatus was reassembled after cleaning. In some cases this would result in a disturbance of the film and hence less cooling. Reproducibility with the 4-inch rough-surface tube was within 8 percent for 17 runs; variations as high as 14 percent were obtained with three other runs.

#### EFFECT OF EXPERIMENTAL VARIABLES ON LIQUID-COOLED LENGTH

In the heat-transfer experiments, data on liquid-cooled length were obtained for independent variations of air temperature, air-mass velocity, coolant flow, tube diameter, and injection method.

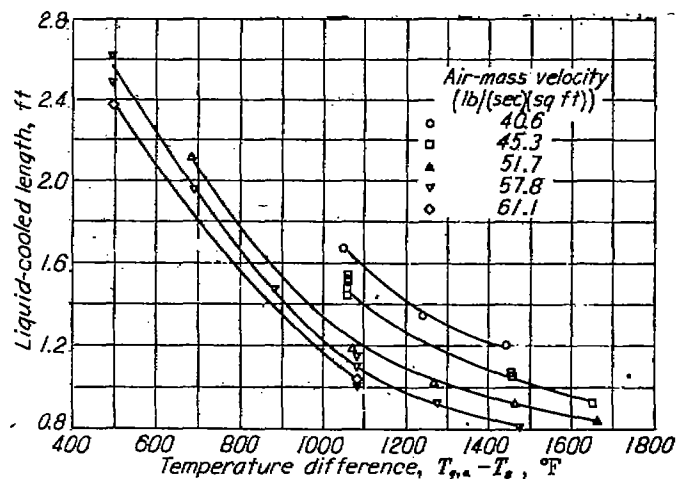


FIGURE 5.—Variation of liquid-cooled length with air to coolant temperature difference and air-mass velocity. Rough-surface tube of 4-inch diameter; air-stream Reynolds numbers,  $4.8$  to  $10 \times 10^5$ ; water flow per circumferential length, 0.123 pound per second per foot.

**Air temperature and mass velocity.**—The effect of air temperature and mass velocity is shown in figure 5, where liquid-cooled length is plotted as a function of the difference between air-stream and coolant-film surface temperatures ( $T_{s,a} - T_s$ ) for various air-mass velocities. As would be expected, the liquid-film-cooled length decreases with either an increase in temperature difference or increase in mass velocity.

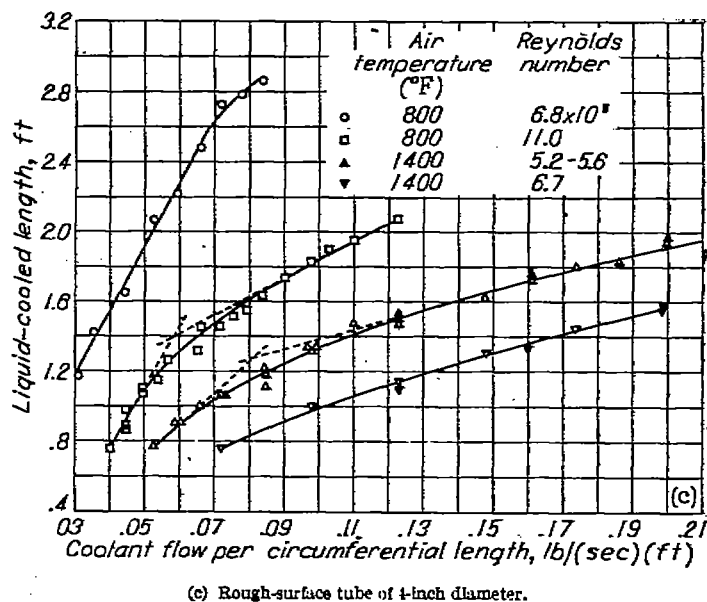
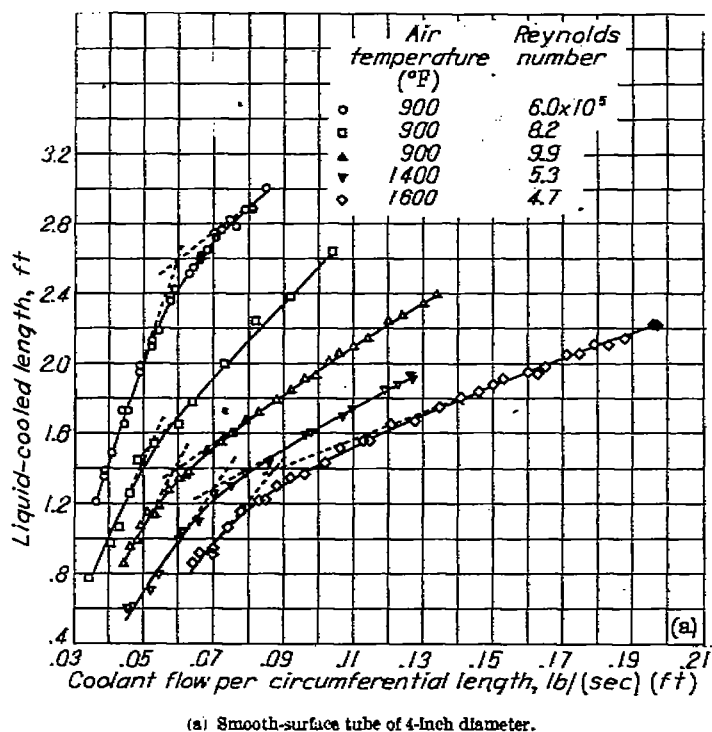


FIGURE 6.—Concluded. Variation of liquid-cooled length with water flow per circumferential length.

are shown in figure 6(a) for three different air temperatures with approximately the same air-mass velocity and for three different air-mass velocities with the same air temperature. For each of the different air-stream conditions, the relation between the liquid-cooled length and the coolant flow per circumferential length is nonlinear and shows the same trends. The cooling effectiveness of a given rate of coolant flow is greatest at the lower coolant flows, decreases appreciably in the range of coolant flow between 0.05 and 0.09 pound per second per foot, and does not change greatly at the higher flows.

Data in the 2-inch tube are shown in figure 6(b). Each of the curves shows the same trends, and the large decrease in cooling effectiveness occurs in the same region of coolant flow per circumferential length as the data of figure 6(a). Data in the 4-inch rough-surface tube are shown in figure 6(c), and the curves show the same trends as those with the smooth-surface tubes. The reason for this nonlinear effect was found, from the visual experiments, to be the formation of wavelike disturbances on the film surface with increasing coolant flow and will be discussed.

**Coolant-injection methods.**—Figure 7 shows a comparison of data obtained with the porous-surface and jet-type injectors; liquid-cooled length is plotted as a function of coolant flow per circumferential length for constant gas-stream conditions. The data show that no significant difference in the amount of cooling was obtained with the two different coolant injectors. With both injectors the coolant was introduced in such a manner as to keep it on the wall and to prevent penetration of the liquid into the gas so that the liquid film could be formed without unnecessary loss of coolant at the injector. The data in figure 7 were obtained with deposits on the inner surface of the rough-surface tube which had been formed during previous experiments and had not been

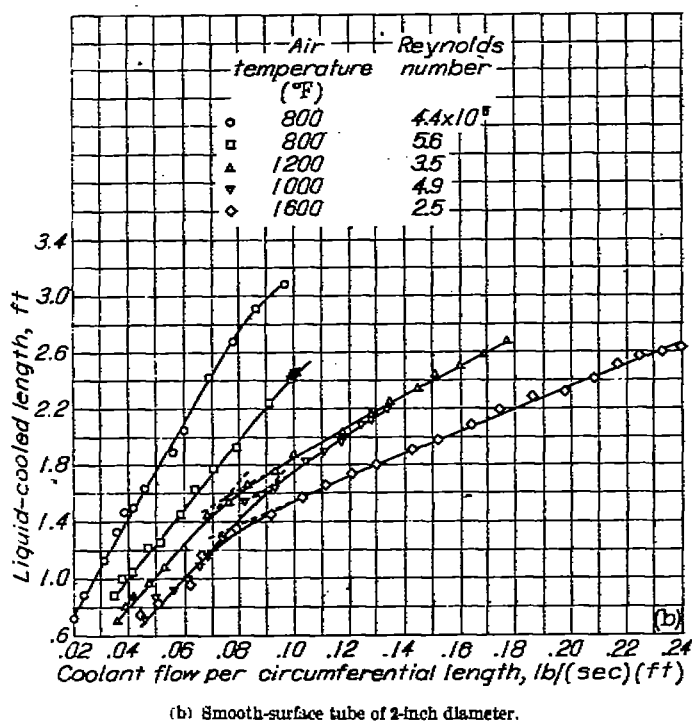


FIGURE 6.—Variation of liquid-cooled length with water flow per circumferential length.

**Coolant flow and tube diameter.**—Analysis of the data with two different tube diameters indicated that the ratio of coolant flow to tube circumference, which is an index of coolant-film thickness, was an independent variable. Figure 6 shows liquid-film-cooled length plotted against this ratio (coolant flow per circumferential length) for various air-stream conditions. Data in the 4-inch smooth-surface tube



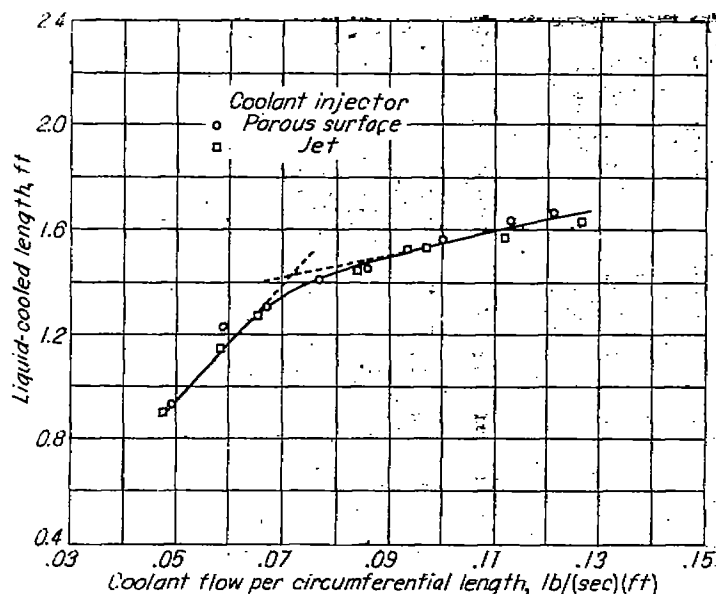


FIGURE 7.—Variation of liquid-cooled length with water flow per circumferential length for different coolant injectors. Rough-surface tube of 4-inch diameter with deposits on surface; air-stream Reynolds number,  $10.7 \times 10^5$ .

removed and therefore are not consistent with the other data obtained with the rough-surface tube. The data are useful for the comparison of coolant injectors because all values were obtained with the tube surface in the same condition.

## RESULTS OF VISUAL FLOW EXPERIMENTS

### VELOCITY AND THICKNESS OF LIQUID FILMS

The liquid films established on the inner surface of the tubes were found in the visual experiments to be very thin for the range of test conditions. Computed values of the liquid-film thickness were from 0.005 to 0.0005 inch with corresponding surface velocities of the liquid film from 10 to 35 feet per second. The symbols and the method used for calculating the liquid-film thickness or velocity are given in appendixes A and B, respectively. The velocities of the disturbances observed on the film surface were measured from the high-speed motion pictures taken at various conditions. These values agreed favorably with the calculated surface velocity of the liquid film for the same conditions.

Experimentally determined velocities of surface disturbances and corresponding thicknesses of liquid films are shown in the following table:

Air-stream Reynolds number	Water flow (lb/(sec)(ft))			
	0.040		0.123	
	Disturbance velocity (ft/sec)	Film thickness (in.)	Disturbance velocity (ft/sec)	Film thickness (in.)
$11.8 \times 10^5$	17.5	0.002	21	0.005
$28.6 \times 10^5$			30	0.003

The effect of gravity on the liquid film, which tends to decrease the film thickness in the upper portion of the

horizontal tubes, was not discernible visually; its magnitude and effects have been discussed previously.

### DESCRIPTION OF WATER-FILM DISTURBANCES

Observations, with the aid of stroboscopic light, of water films on the inside surface of transparent tubes revealed changes in the appearance of the flow for different water flows. With constant air-stream conditions, the water flow appeared essentially smooth at low water flows; whereas there were disturbances having the appearance of waves on the water surface at higher water flows. The change in the appearance of the water flow occurred gradually as the water flow increased; figure 8 shows shadowgraph pictures of the flow for increasing water flows. The photographs are arranged to show three regions involved in the changing appearance of the water flow as the flow increases: (1) smooth flow (no appreciable disturbance), (2) transition from small traces of disturbance to appreciable and consistent clearly visible disturbances, and (3) increasing number and magnitude of disturbances. Although there was a gradual change from undisturbed to disturbed flow, liquid flows that define the transition region at given flow conditions could be determined by two or more observers with good agreement. The degree of disturbance continues to increase with increased liquid flow after the transition region.

### EFFECT OF FLOW VARIABLES ON LIQUID-FILM CHARACTERISTICS

Experiments were conducted to determine the effect of several variables on the values of liquid flow per circumferential length over which the flow transition occurred and on the appearance of the surface. The variables investigated were air-mass velocity (or Reynolds number), tube diameter, air temperature, liquid viscosity, and liquid surface tension. The values of liquid flow per circumferential length defining the transition region for the different flow conditions are given in tables IV and V.

**Effect of air-mass velocity.**—The liquid flows defining the transition region with water are given in table IV for different air-mass velocities at ambient temperature with the aid of three different transparent tubes. The water flows per circumferential length over which the flow transition occurred did not change appreciably over the air-mass velocity (or Reynolds number) range. The disturbances had different appearances at the various air-mass velocities, being smaller and more numerous at the higher air-mass velocities. A comparison between the pyrex and clear plastic tubes (table IV) shows that the transition region for the plastic tube starts at a flow about 25 percent lower than that for the pyrex tube. Both tube surfaces were essentially smooth; the difference was probably due to different surface characteristics of the materials.

**Effect of tube diameter.**—The transition region for several air-mass velocities (or Reynolds numbers) with 2- and 4-inch-diameter plastic tubes is also shown in table IV. The results show no appreciable difference in the transition region (liquid flow per circumferential length) for the two tube diameters, and the disturbances had the same appearance for corresponding air-mass velocities.



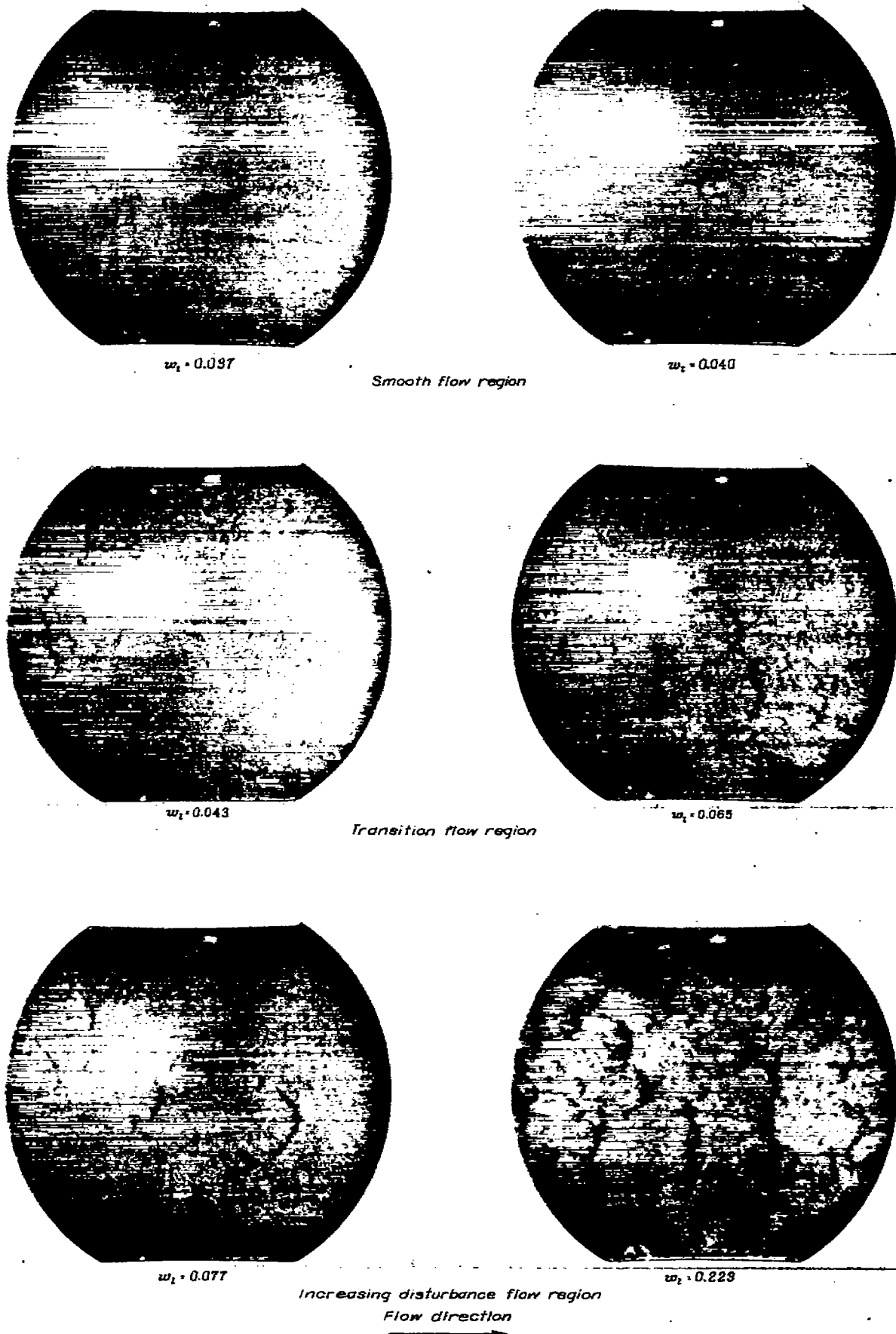
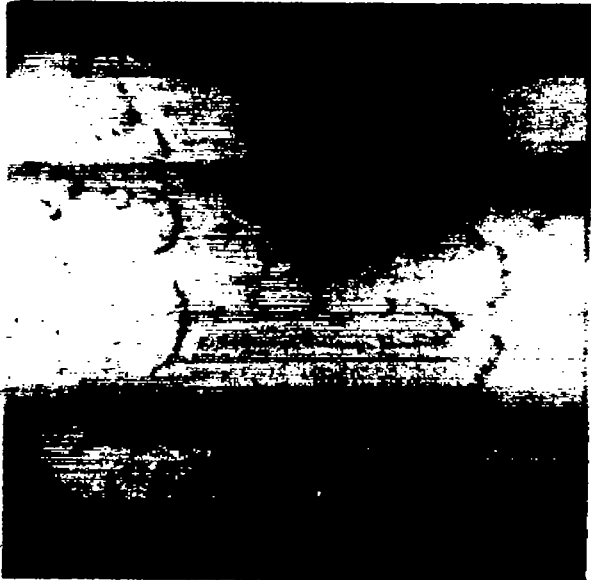


FIGURE 3.—Shadowgraphs of water films with cocurrent air flow in horizontal tube. Clear plastic tube of 4-inch diameter; air-stream Reynolds number,  $11.8 \times 10^4$ ; air temperature,  $80^\circ \text{F}$ ; liquid flow  $w_t$ , pounds per second per foot of circumference.



(a)



(b)

(a) Clear plastic tube of 4-inch diameter; air temperature, 80° F; air-stream Reynolds number,  $11.8 \times 10^4$ ; water flow, 0.093 pound per second per foot.  
(b) Pyrex tube of 4-inch diameter; air temperature, 800° F; air-stream Reynolds number,  $6.6 \times 10^4$ ; water flow, 0.130 pound per second per foot.

FIGURE 9.—Shadowgraphs of water films with cocurrent air flow in horizontal tube at different air temperatures.

**Effect of air temperature.**—Significant information on the effect of air temperature on the transition region could not be obtained because water-flow rates in this region were too small to form a liquid film along the entire length of the

tube at high air temperature and thus prevent overheating of the tube.

However, the effect of temperature on the flow disturbances accompanying high rates of water flow was observed. For example, figure 9 shows shadowgraph pictures of the water flow for air temperatures of 80° and 800° F for the same air flow. The pictures indicate, as did visual observations, that the disturbances had the same appearance at the different air-stream temperatures; apparently there is no boiling or appreciable effect on the liquid-film surface due to vaporization.

**Effect of liquid viscosity.**—Variation of liquid viscosity and surface tension was obtained by using water, water—ethylene glycol solutions, and water-detergent solutions at constant temperatures. The properties of the solutions that were used are listed in table I.

The liquid-flow disturbances with aqueous glycol solutions were less wavelike in appearance, smaller in size, and less distinct with increased viscosity. Definition of a transition region, as obtained with water, was difficult because of the gradual development of the disturbances with increased liquid flow. However, as viscosity was increased, higher liquid flows were required before appreciable disturbances were observed.

**Effect of surface tension.**—In table V are shown an increase in the liquid flows for the start of the transition region and an increase in the magnitude of the transition-flow region for decreases in liquid surface tension. The transition region for the 0.095-percent detergent solution (surface tension, 50 percent of that for water) starts at a liquid flow about 20 percent higher than that for water, and the magnitude of the transition flow region is about twice as large as that for water. The physical characteristics of the flow of water-detergent solutions were essentially the same as observed with water except when the detergent concentration was sufficient to reduce the surface tension below approximately one half that of water. Then the following liquid-flow characteristics were observed: (1) At low liquid flows, small areas of roughened surface appeared; and (2) as the liquid flow was increased, the disturbances became more numerous and intense, covering the entire surface. The disturbances, however, did not have the wavelike appearance that was observed with water.

RELATION BETWEEN DISTURBANCES AND FLOW CONDITIONS

By analysis, the surface disturbances or turbulence of the liquid film was found to originate when the liquid film was thick enough to enter the flow region where turbulent forces predominate over viscous forces. Plots of the generalized velocity distribution for fully developed flow in smooth tubes, as given in references 17 and 18, are shown in figure 10, and this distribution is assumed applicable to the liquid film. The flow regions where the viscous or turbulent forces predominate are defined by the value of the wall-distance parameter  $y^+$ . Viscous forces predominate in the laminar layer ( $y^+ < 3$ ); turbulent forces, in the turbulent core ( $y^+ > 30$ ); and both laminar and turbulent forces are present in the intermediate region ( $3 < y^+ < 30$ ) (references 17 and 18).

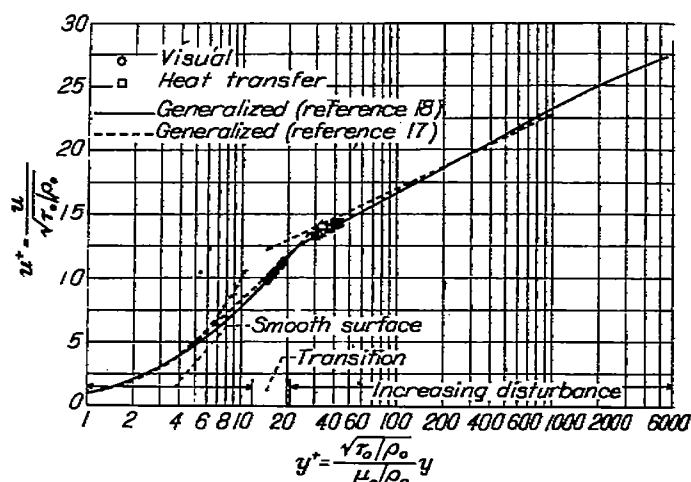


FIGURE 10.—Association of visual flow regions and heat-transfer results with generalized velocity distribution for fully developed flow in smooth tubes applied to liquid films.

For the purposes of this investigation, it is convenient to place the results in terms of  $w^+$ , a flow-rate parameter, because the flow of the liquid was measured for each run. This flow-rate parameter, which is the integral of the curve of  $u^+$  against  $y^+$  (fig. 10), is derived in appendix B.

Values of the flow-rate parameter  $w^+$  were calculated for the median liquid flows defining the transition region as listed in tables IV and V; the viscosity of the liquids at 80° F (temperature when introduced into tube) was used. The corresponding values of  $y^+$  were obtained from figure 11, which is a graphical integration of the curve of figure 10 for various values of  $y^+$  (appendix B). These values are plotted on the generalized velocity distribution of figure 10. The highest and lowest values of  $y^+$  defining the transition region as obtained from tables IV and V are also shown in figure 10 by solid lines, and the data indicate that the observed transition region for the various conditions occurred over the region of  $w^+=50$  to  $w^+=150$  or  $y^+=12$  to  $y^+=21$ . The previously defined flow regions as shown in figure 7 may be associated with figure 10 as follows: At values of  $y^+ < 12$ , the liquid film appears relatively smooth. In the region  $12 < y^+ < 21$ , a surface disturbance developed on the liquid film. For values of  $y^+ > 21$ , the disturbance increases with  $y^+$  to the limit of the experimental conditions at  $y^+=80$ . The approximate liquid flow at which the surface disturbances initially occur can be obtained with a flow-rate parameter  $w^+$  of 90, which corresponds to  $y^+=15$ .

#### RELATION BETWEEN HEAT-TRANSFER DATA AND LIQUID-FILM DISTURBANCES

Analysis of the occurrence of liquid-film disturbances was applied to film-cooling heat-transfer results shown in figure 6, where cooling effectiveness is shown as a function of water flow for different hot-air-stream conditions. Values of the flow-rate parameter  $w^+$  were determined for water flows representing medians (indicated by the intersection of the dashed lines) over which marked changes in cooling effectiveness occurred for each of the curves in figure 6, and which were suspected to correspond to the initial occurrence of liquid-film disturbances. The viscosity of water at 210° F

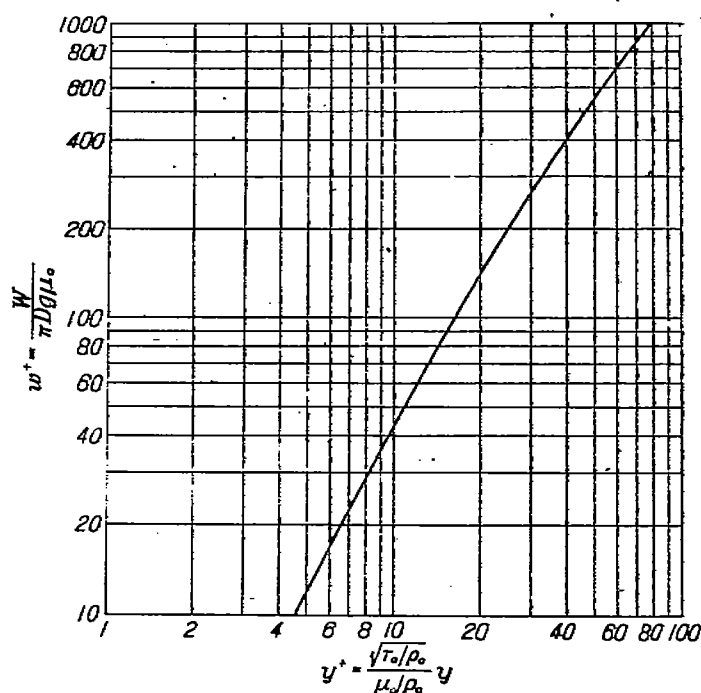
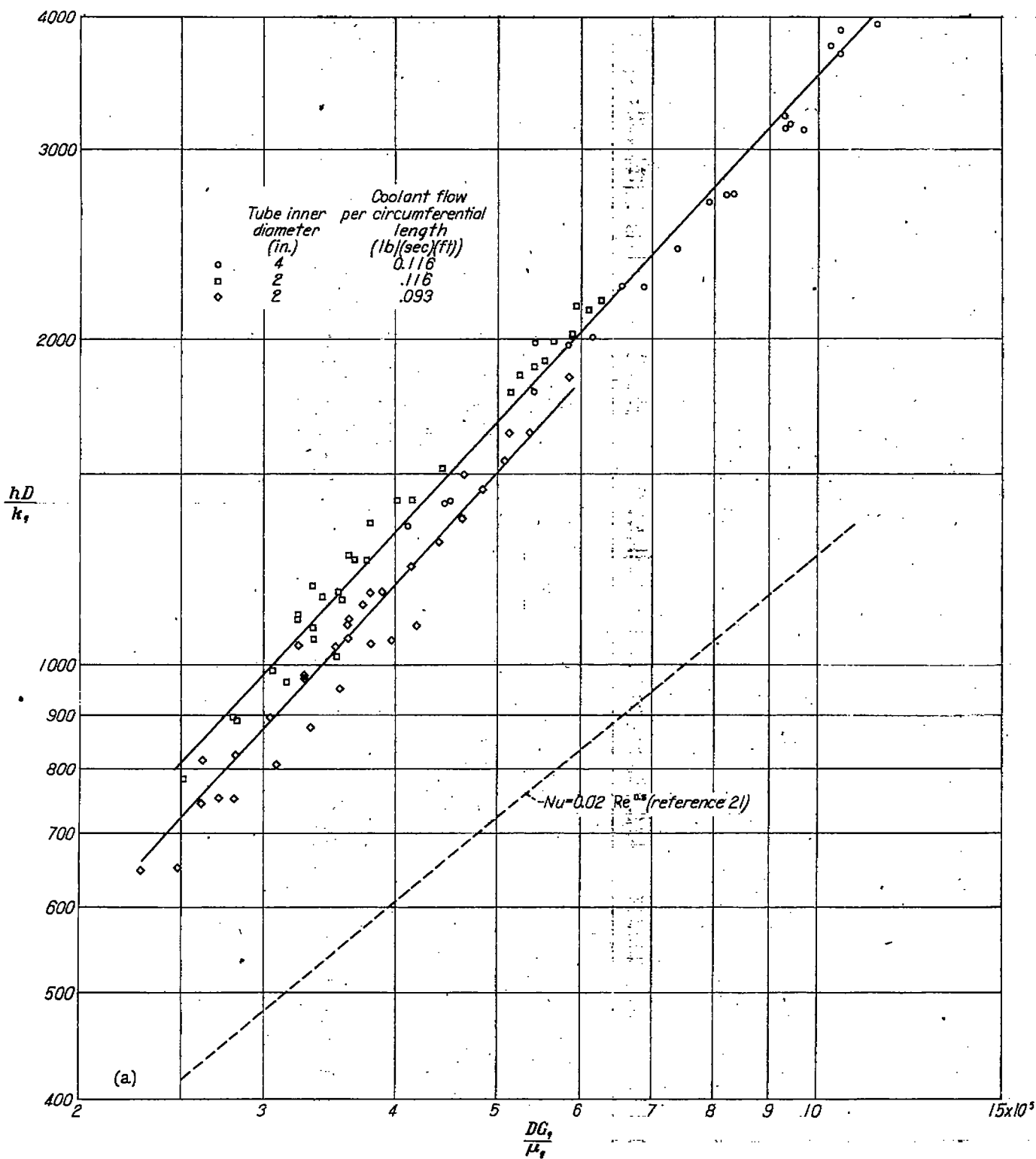


FIGURE 11.—Variation of dimensionless flow-rate parameter with wall-distance parameter.

(estimated average temperature of water film) was used. Values for  $w^+$  varied between 266 and 448 and the corresponding values of  $y^+$  as plotted on figure 10 varied between 30 and 44; these are higher values than obtained for the transition region from the visual observations. This result would be expected because of the differences in the two systems. The visual results were obtained with ambient-gas-stream temperature; thus no appreciable evaporation of the liquid into the gas stream occurred, and the thickness of the liquid film was essentially constant downstream of the injection point. In the heat-transfer investigations, however, liquid was evaporating from the liquid film and the thickness decreased along the duct. Thus the two systems can be compared only at a point where, in the heat-transfer case, no liquid has been lost to the gas stream, which would be the injection point. For the visual observations where the thickness of the liquid film is constant along the duct, disturbances take place along the entire duct when the initial thickness is sufficient for a surface disturbance to occur. In the heat-transfer investigations, however, the thickness decreases along the duct and this decrease would tend to stabilize any disturbances of the film surface. Thus for the same value of  $y^+$  and the same initial liquid flow, the liquid-film surface would be more turbulent in the visual observations than in the heat-transfer investigations. By assuming the average thickness of the liquid film to be one half the initial thickness for the heat-transfer case, the determined value of  $y^+$  is reduced by a factor of 2 (from that for no evaporation) and the heat-transfer results are in agreement with the visual results. The approximate flow at which the effectiveness of water changes in a film-cooling application is obtained with a flow-rate parameter  $w^+$  of 360, which corresponds to  $y^+=37$ .



(a) Smooth-surface tubes of 2- and 4-inch diameter. Air temperatures, 800° to 2000° F; air-mass velocities, 39.4 to 81.7 pounds per second per square foot.

FIGURE 12.—Correlation of heat transfer from air stream to water film at constant coolant flow per circumferential length.

ANALYSIS OF HEAT-TRANSFER DATA

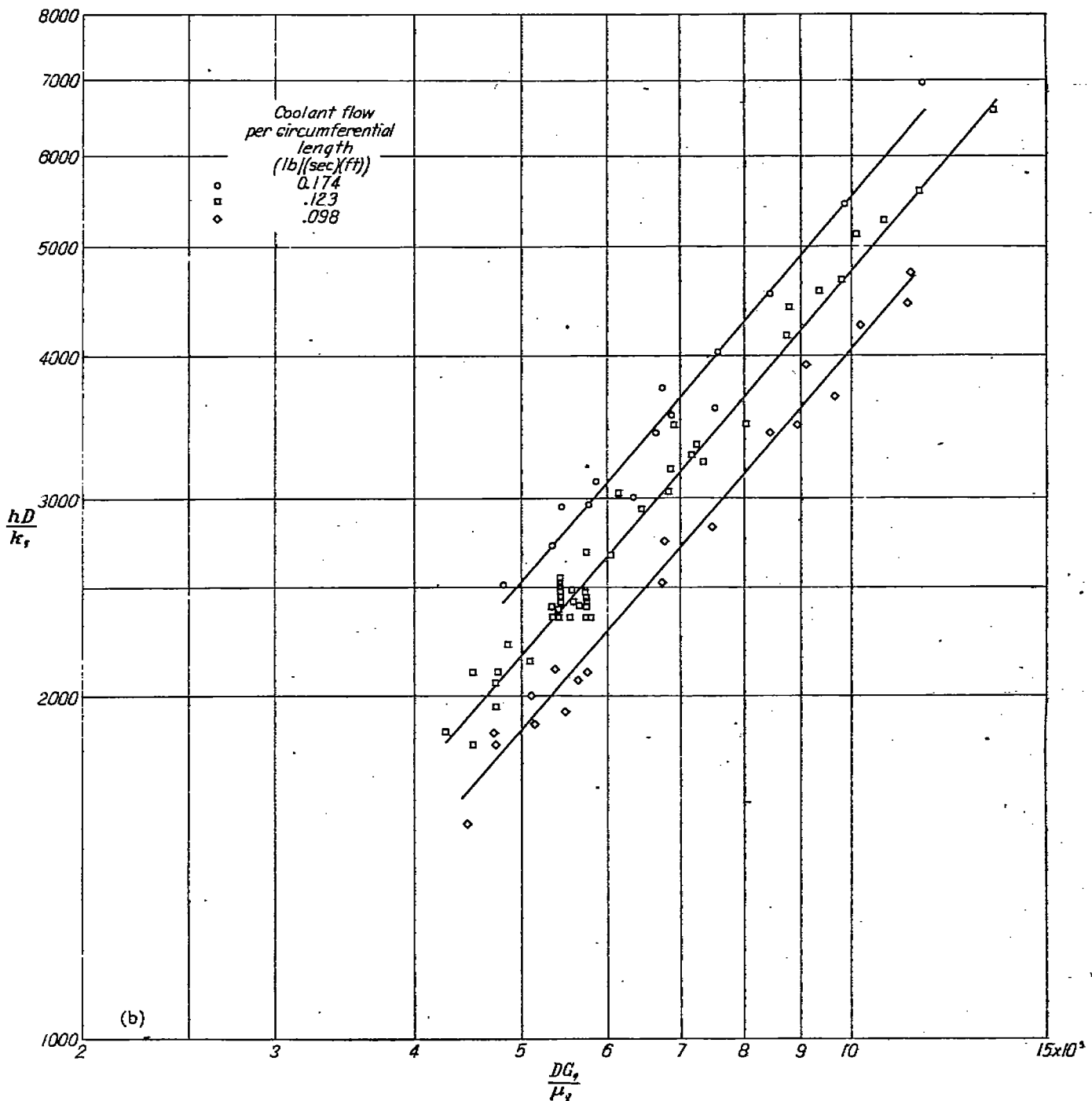
The data were generalized in a form convenient for determining film-coolant requirements even though a complete correlation was not obtained because of the changing condition of film-coolant flow with changes of coolant-flow rate.

CORRELATION OF HEAT TRANSFER FOR CONSTANT COOLANT FLOW PER CIRCUMFERENTIAL LENGTH

In figure 1 is shown a schematic representation of the liquid film vaporizing in the air stream. Heat is transferred

from the hot-air stream to the coolant film and, simultaneously, mass transfer from the coolant to the air occurs as the coolant vaporizes.

The method used to correlate the data was to consider heat transfer as the controlling process, and the driving force or temperature difference was taken between average air-stream temperature and the liquid surface temperature, which was approximated by assuming it to be at boiling temperature. Mass-transfer equations did not provide a



(b) Rough-surface tube of 4-inch diameter. Air temperatures, 600° to 2000° F; air-mass velocities, 39.7 to 81.5 pounds per second per square foot.

FIGURE 12.—Concluded. Correlation of heat transfer from air stream to water film at constant coolant flow per circumferential length.

successful method of relating the data because their use required a more accurate determination of liquid surface temperature than was feasible.

Average heat-transfer coefficients for each run were calculated by the following heat balance across the air-coolant-vapor film:

$$h = \frac{W_c [C_{p,c}(T_s - T_l) + H_s]}{(T_{s,a} - T_s)(\pi DL)} \quad (1)$$

The following equation correlated the data for constant values of coolant flow per circumferential length:

$$Nu = a(Re)^*$$

A more complete equation for correlating film-cooling data may also include the dimensionless groups  $Pr$ ,  $Sc$ , and  $k_s/k_f$ . These parameters are not included because they were essentially constant for the conditions of the experiments. The latter two parameters predicted the effects of diffusion of vapor into the gas stream on heat-transfer coefficients for the data of reference 12.

The Nusselt number for each run was calculated from the experimental heat-transfer coefficient, the diameter of the

tube, and the thermal conductivity of air at the average bulk temperature of the air stream ( $T_{s,a}$ ). Air-stream Reynolds numbers were calculated for each run by means of tube diameter, air-mass velocity, and viscosity of air at average bulk temperature  $T_{s,a}$ .

The log-log plots of Nusselt numbers against Reynolds numbers for several different values of coolant flow per circumferential length are shown in figure 12. All the data shown in figure 12 were obtained with coolant flows large enough to cause cooling-film disturbances; correlation could not be investigated over a large range of air flows and temperatures with low coolant flows which did not cause film disturbances because, at the high air flows and temperatures of the experiments, liquid-cooled lengths were too small to be accurately measured.

In figure 12(a) are shown data obtained in both 2- and 4-inch-diameter smooth-surface tubes at a coolant flow of 0.116 pound per second per foot of tube circumference. The slope of the line drawn for these data is approximately 1.05. Also shown in figure 12(a) are data in the 2-inch smooth-surface tube at a coolant flow of 0.093 pound per second per foot of tube circumference; although there is considerable scatter, the slope of the line for these data appears to be approximately the same as that for the data at the other coolant flow. Comparison of data in the 2-inch tube at two different coolant flows shows that heat-transfer coefficients were higher with the higher coolant flow. A conventional relation for heat transfer from flowing hot gases to tube walls without film cooling is represented in figure 12(a) by a dashed line; the experimentally determined coefficients for film cooling are considerably greater.

Data obtained in the 4-inch rough-surface tube at three different coolant flows are presented in figure 12(b). The slopes of the lines for the data at each of the different coolant flows are approximately 1.07, and the heat-transfer coefficients increase with increased coolant flow. A comparison of data from figures 12(a) and 12(b) shows that heat-transfer coefficients are approximately 20 percent higher with the rough-surface tube than with the smooth-surface tube.

Data scatter for the correlations presented in figure 12 is of the same order of magnitude as reproducibility of liquid-cooled length with constant test conditions.

#### GENERALIZED PLOT OF HEAT-TRANSFER DATA

The data of figure 6 showed that the surface area cooled by a given flow of coolant decreased with increased coolant flow. The visual experiments indicated that the decreased effectiveness of the coolant resulted from the formation of wavelike disturbances on the liquid film. Figure 12 shows that, although the heat transfer from the hot air to the liquid film is correlated for constant values of coolant flow per circumferential length, the heat-transfer coefficients increase with increased coolant flow per circumferential length.

In order to generalize all the film-cooling data on a single plot, the equation for heat transfer plotted in figure 12 was used. This equation is

$$\frac{hD}{k_s} = a \left( \frac{DG_s}{\mu_s} \right) \quad (2)$$

where the value of  $a$  can be considered to vary with coolant flow per circumferential length. The Reynolds number exponent was taken as unity for convenience because accuracy of the data did not permit closer determination. Substituting the equation for heat-transfer coefficient (equation (1)) in equation (2) and rearranging yield:

$$\frac{W_c}{\pi D} \sim \frac{Lk_s(T_{s,a} - T_s)}{D(\Delta H)} (Re)_s \quad (3)$$

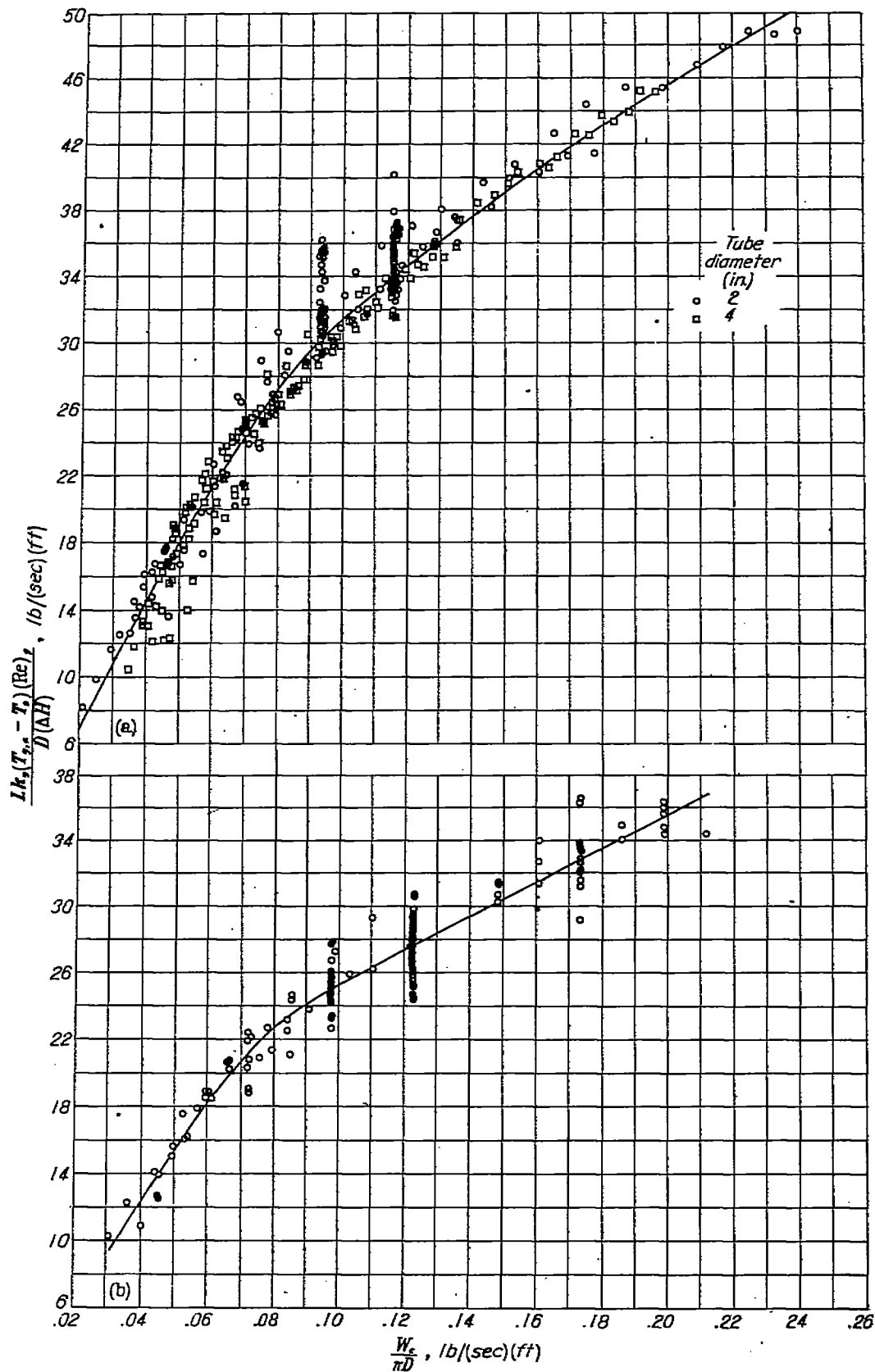
In figure 13(a) is shown this relation plotted for data obtained with the smooth-surface tubes; coolant flow per circumferential length of tube is plotted against liquid-cooled length and gas stream and coolant variables. Figure 13(b) shows the relation plotted for data obtained with the 4-inch rough-surface tube. A comparison of the data shown in figure 13(a) with those in figure 13(b) shows that the amount of cooling in the rough-surface tube was about 20 percent less than in the smooth-surface tubes. Less cooling was obtained in the rough-surface tube because surface roughness, projections, and holes on the inner surface all tend to disrupt the liquid film and promote loss of coolant from the wall. Quantitative measures of the effects of surface roughness and of the other surface interruptions on the amount of cooling obtained could not be made because the surface irregularities in the rough-surface tube were not well defined. The curves of figure 13(a) and 13(b) show the same trends as the curves of figure 6; cooling effectiveness per pound flow of coolant decreases appreciably in the range of water flow between 0.05 and 0.09 pound per second per foot.

#### DISCUSSION

The water flow required to maintain liquid-film cooling over a desired area in a smooth-surface straight tube with fully developed, turbulent air flows to 2000° F entering the tube can be determined from figure 13(a). Figure 13(a) is also useful for estimating film-coolant requirements for conditions which have not been investigated experimentally and for acting as a guide to correlate data obtained from actual applications.

Further research is required to determine the effects on film-cooling results of: (1) gas temperatures higher than 2000° F, (2) coolant properties which affect the flow conditions of the liquid film, (3) the mass diffusion from the liquid film, (4) gas-stream pressure, (5) gas-flow conditions differing from the well-controlled conditions of the experiments, (6) the use of reactive coolants, and (7) changing contour of the flow duct.

Additional data are required to determine if gas temperatures greater than 2000° F will alter results, as predicted from figure 13, other than that accountable to radiation. Coolant requirements obtained from figure 13 account for the heat transferred from the hot gas to the liquid film by forced convection alone and not by radiation to the liquid film or



(a) Smooth-surface tubes. Air temperatures, 800° to 2000° F; air-stream Reynolds numbers, 2 to  $11 \times 10^4$ .

(b) Rough-surface tube of 4-inch diameter. Air temperatures, 600° to 2000° F; air-stream Reynolds numbers, 4 to  $14 \times 10^4$ .

FIGURE 13.—Generalized plots of film-cooling data based on correlation of heat transfer from air stream to water film. Static pressures, 42 to 74 inches of mercury absolute; air-mass velocities, 39.4 to 81.7 pounds per second per square foot.



to the tube wall; where the heat transferred by radiation is appreciable, additional coolant is required. If the amount of heat transferred to the tube wall by radiation were large enough to result in a wall temperature considerably above the saturation temperature of the coolant, it is possible that additional coolant will be lost because of the disturbance of the liquid film caused by the formation of vapor bubbles under the film.

Additional data are needed on the effects of coolant properties. Results predicted from figure 13(a) may differ from those obtained with coolants having viscosities and surface tensions considerably different from those of water on account of the effect of these properties on the flow conditions of the liquid film. The visual flow experiments showed that the changing flow conditions of the liquid film with increased values of liquid flow per circumferential length (evidenced by the occurrence of turbulent or disturbed flow) result in the variation in cooling effectiveness with increased coolant flow which can be seen in figure 6. The experiments also showed that the values of coolant flow per circumferential length at which disturbed flow begins, and the nature of the disturbed flow, differ with the viscosity and surface tension of the liquid.

Further research is required to investigate the effects of diffusion of vapor from the liquid film. As discussed previously, the data of reference 12 were correlated by considering heat transfer as the controlling process and the effects of simultaneous mass diffusion were predicted by the parameters  $Sc$  and  $k_g/k_s$ . Additional experiments with large changes of coolant and gas properties are required to determine the importance of these parameters in the case of film cooling.

Effects of gas-stream pressure on the evaporation of the liquid film, other than predicted by the Reynolds number, should also be investigated by additional experiments. The variation of pressure occurring in the experiments reported herein resulted from the method of controlling the air flow and the temperature; independent investigation of pressure as a variable was not made.

Gas-flow conditions with many applications of film cooling are considerably different from those of the experiments reported herein, and large differences between the film cooling obtained in such cases and that obtained in the experiments are possible. For example, in a rocket-engine combustion chamber, the effects of the combustion process and the short length of chamber will not allow conditions approximating fully developed, turbulent velocity and temperature distributions as with the experiments.

An example is given in appendix C to illustrate the use of figure 13(a) for determining film-coolant requirements.

Because wavelike disturbances occur on a liquid-cooling film when the coolant flow per circumferential length of the tube exceeds a certain value, and the result is a decrease in film-cooled area per unit flow of coolant, it may be desirable in many practical applications to limit the coolant flow introduced at any one axial position and to introduce it at several positions over the area to be cooled in order to

achieve the desired cooling with as little coolant flow as possible.

In general, because an internal-film coolant cannot be recirculated and must be carried as additional weight in flight, the application of film cooling in flight-propulsion engines appears limited either to conditions where propulsive energy is derived from the film coolant in addition to its cooling function or to conditions of high heat release where more conventional cooling methods are inadequate. The use of film cooling in some rocket engines is an example of the application in which both of these conditions apply.

## SUMMARY OF RESULTS

### HEAT-TRANSFER EXPERIMENTS

An investigation of film cooling was conducted in 2- and 4-inch-diameter straight tubes with air flows at temperatures from 600° to 2000° F and diameter Reynolds numbers from 2.2 to  $14 \times 10^5$ . The film coolant, water, was uniformly injected around the circumference at a single axial position on the tube at flow rates from 0.02 to 0.24 pound per second per foot of tube circumference (0.8 to 12 percent of the air flow). Liquid-cooled lengths were determined by means of wall-temperature measurements. The results of the experiments are summarized as follows:

1. Liquid-coolant films were established and maintained around and along the tube wall in cocurrent flow with the hot gas.

2. The tube wall was kept below the boiling temperature of the coolant over the surfaces covered by liquid coolant; downstream of the point at which the liquid film ceased because of vaporization, little additional cooling of the tube was obtained.

3. The relation between liquid-cooled length and coolant flow for given gas-stream conditions was nonlinear; the effectiveness of a given flow rate of coolant introduced at a single axial position on the tube decreased with increased coolant flow.

4. The film-cooling data were generalized by means of a heat-transfer relation and data obtained over a range of coolant flows; this generalization of data facilitates the estimation of the flow rate of inert coolant required to maintain liquid-film cooling over a given area of tube surface when the gas-stream conditions are known.

### VISUAL FLOW EXPERIMENTS

Visual observations and flow analyses were made of annular liquid films in cocurrent flow with air in 2- and 4-inch-diameter horizontal transparent tubes. The investigations were conducted with air temperatures of 80° and 800° F and Reynolds numbers from 4.1 to  $29 \times 10^4$ . Liquid flows of water, water-detergent solutions, and aqueous ethylene glycol solutions were investigated at flows in the same range as the heat-transfer experiments. The results are summarized as follows:

1. For the range of conditions investigated, the velocity of the liquid-film surface varied from approximately 10 to 35 feet per second with corresponding liquid-film thicknesses of 0.005 to 0.0005 inch.

2. The liquid flow was relatively smooth until the liquid-flow rate was sufficiently high so that the liquid annulus was thick enough to enter the region where turbulent forces predominate over viscous forces; wavelike disturbances then developed on the liquid film. Approximate liquid-flow rate for this transition could be predicted.

3. The liquid flow per circumferential length at which liquid-flow disturbances initially occurred increased with increased liquid viscosity, increased slightly with decreased liquid surface tension, and did not vary appreciably with changes in air-mass velocity.

4. Liquid-flow disturbances had different appearances with different air-mass velocities, liquid viscosities, and liquid surface tensions; in general, the size and the number of disturbances varied.

5. Visual observations at several air temperatures between ambient and 800° F indicated no boiling or appreciable disturbance on the liquid film due to vaporization of the liquid.

### CONCLUSIONS

The following conclusions are made from experiments in which tubes containing flowing hot air were cooled by water films on the inner surfaces and from visual observations and analysis of the liquid flow in such films:

1. A liquid-cooling film can be established and maintained on the inner surfaces of a tube through which high-velocity hot gases are flowing by introducing the liquid coolant onto the inner surface about the tube circumference; the gases sweep the coolant downstream, resulting in an annular flow of liquid coolant.

2. Tube-wall temperatures are maintained at or near the boiling temperature of the water over the surfaces covered by liquid; little additional cooling of the tube is obtained downstream of the point at which the liquid film ceases because of vaporization.

3. The liquid-coolant film is relatively smooth unless the coolant-flow rate is sufficiently high that the liquid annulus is thick enough to enter the flow region where turbulent forces predominate over viscous forces; wavelike disturbances then develop on the liquid film. These disturbances result in increased loss of coolant from the film and reduce effectiveness of the coolant.

4. Prediction can be made of the approximate highest coolant flow which can be introduced at a single axial position in a tube to form a liquid film without the effectiveness of the coolant being reduced by the formation of disturbances.

5. In order to film cool a given surface area with as little coolant flow as possible, it may be necessary to limit the flow of coolant introduced at any single position and to introduce it at several positions.

6. The rate of flow of inert coolant required to maintain liquid-film cooling over a given area of tube surface can be estimated with the aid of a generalized plot of film-cooling data when the gas-stream conditions are known.

LEWIS FLIGHT PROPULSION LABORATORY,  
NATIONAL ADVISORY COMMITTEE FOR AERONAUTICS,  
CLEVELAND, OHIO, May 27, 1952.

## APPENDIX A

### SYMBOLS

The following symbols are used in this report:

$A$	cross-sectional area of film-cooled tube, sq ft
$\sigma$	proportionality constant
$C_p$	average specific heat at constant pressure, Btu/(lb) (°F)
$D$	inside diameter of tube, ft
$d$	volumetric diffusion coefficient or diffusivity, sq ft/sec
$G$	mass velocity, lb/(sec)(sq ft)
$g$	acceleration due to gravity, 32.2 ft/sec <sup>2</sup>
$H_i$	heat of vaporization of coolant at $T_{s,1}$ , Btu/lb
$\Delta H$	change in enthalpy of liquid coolant from entering condition through vaporization, Btu/lb
$h$	heat-transfer coefficient, Btu/(sec)(sq ft)(°F)
$k$	thermal conductivity, Btu/(sec)(sq ft)(°F/ft)
$L$	liquid-cooled length, ft
$p$	static pressure, lb/sq ft abs
$T_s$	gas-stream bulk temperature
$T_{s,1}$	stagnation temperature of gas stream entering film-cooled tube, °F
$T_{s,2}$	stagnation temperature of equilibrium gas-coolant vapor mixture, °F

$T_{s,g}$	arithmetic mean stagnation temperature of the gas stream, $\frac{T_{s,1} + T_{s,2}}{2}$ , °F
$T_i$	temperature of coolant before injection, °F
$T_s$	temperature of liquid-coolant surface (assumed at saturation temperature), °F
$u$	velocity parallel to axis of tube, ft/sec
$u_b$	bulk or average velocity at cross section of tube, ft/sec
$\dot{W}$	flow rate, lb/sec
$w$	flow rate per unit length, lb/(sec)(ft)
$x$	axial distance from liquid injector, ft
$y$	distance from tube wall, ft
$\mu$	viscosity, lb/(sec)(ft)
$\mu_w$	absolute viscosity of fluid at wall, lb-sec/sq ft
$\rho$	mass density, lb-sec <sup>2</sup> /ft <sup>4</sup>
$\rho_b$	bulk or average mass density at cross section of tube, lb-sec <sup>2</sup> /ft <sup>4</sup>
$\rho_w$	mass density of fluid at wall, lb-sec <sup>2</sup> /ft <sup>4</sup>
$\tau_w$	shear stress in fluid at wall, lb/sq ft
$\omega$	density, lb/cu ft

## Subscripts:

$c$	liquid coolant
$fr$	on friction pressure gradient
$g$	gas
$l$	liquid
$v$	coolant vapor

## Superscript:

$n$	any exponent
-----	--------------

## Dimensionless parameters:

$f$  friction factor,  $-D \frac{(dp)}{dx} \frac{1}{2\rho_b u_b^2}$

$Nu$	Nusselt number, $hD/k$
$Pr$	Prandtl number, $C_p \mu/k$
$Re$	Reynolds number, $DG/\mu$
$Sc$	Schmidt number based on mass diffusivity of vapor, $\mu/\omega_s d$
$u^+$	velocity parameter, $\frac{u}{\sqrt{\tau_o/\rho_o}}$
$w^+$	flow-rate parameter, $\frac{W}{\pi D g \mu_o}$
$y^+$	wall-distance parameter, $\frac{\sqrt{\tau_o/\rho_o}}{\mu_o/\rho_o} y$

## APPENDIX B

## CALCULATION OF VELOCITY AND THICKNESS OF LIQUID FILM AND DERIVATION OF FLOW-RATE PARAMETER

## CALCULATION OF VELOCITY AND THICKNESS OF LIQUID FILM

For annular liquid flow with cocurrent gas flow in a horizontal duct, the velocity or the thickness of the annular liquid film can be calculated by use of the dimensionless parameters  $u^+$  and  $y^+$  and figure 10, which were obtained from references 17 and 18.

**Velocity calculation.**—The parameter  $u^+$  is defined as

$$u^+ = \frac{u}{\sqrt{\frac{\tau_o}{\rho_o}}} \quad (B1)$$

The friction velocity  $\sqrt{\tau_o/\rho_o}$  for a homogeneous fluid flowing in a duct is given by the equation

$$\sqrt{\tau_o/\rho_o} = u_b \sqrt{f/2} \quad (B2)$$

For annular liquid flow with cocurrent gas flow, however, equation (B2) must be modified. This modification is accomplished by referring the friction velocity  $\sqrt{\tau_o/\rho_o}$  to the liquid annulus and by considering the gas flow to be replaced by a fictitious flow of the same liquid as in the annulus. Then the restriction is imposed that the pressure drop per unit length must be the same for the fictitious liquid flow as for the gas flow with the friction factor  $f$  for the actual conditions applying to each case. This restriction means that the dynamic pressures of the fictitious liquid flow and gas flow must be equal or

$$u_{b,l} = \sqrt{\frac{\rho_{b,g}}{\rho_{b,l}}} u_{b,g}$$

Substituting for the velocity in equation (B2) and combining the result with equation (B1) give the following relation for the liquid surface velocity:

$$u_i = u^+ \sqrt{\frac{f}{2}} \sqrt{\frac{\rho_{b,g}}{\rho_{b,l}}} u_{b,g} \quad (B3)$$

**Thickness calculation.**—The parameter  $y^+$  is defined as

$$y^+ = \frac{\sqrt{\tau_o/\rho_o}}{\mu_o/\rho_o} y \quad (B4)$$

Again, referring the expression for  $y^+$  to the liquid annulus and expressing the friction velocity  $\sqrt{\tau_o/\rho_o}$  in terms of the gas-stream velocity give the following relation for the liquid-film thickness:

$$y_i = y^+ \frac{\mu_{o,l}}{\rho_{o,l}} \sqrt{\frac{2}{f}} \sqrt{\frac{\rho_{b,l}}{\rho_{b,g}}} \frac{1}{\mu_{b,g}} \quad (B5)$$

All the variables appearing in equations (B3) and (B5) except friction factor are known for any given conditions. The friction factor for annular liquid flow with cocurrent gas flow is unavailable from experimental data for the range of conditions investigated in this report. Extrapolation of the data in references 13 and 14 indicates that the friction factor for the conditions reported herein is of the order of two to four times that of single-phase flow in a smooth duct for the same gas-stream Reynolds number.

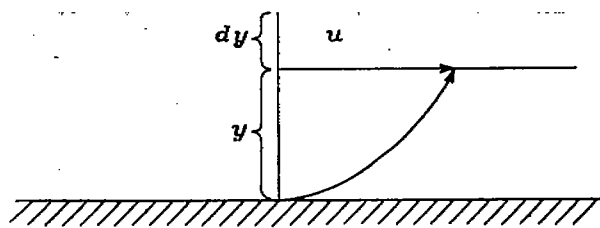
For convenience, a flow-rate parameter defined as  $w^+ = W/\pi D g \mu_o$  (equation (B8)) is used for the calculation. It is the integral of the curve of figure 10 and is plotted as a function of  $y^+$  in figure 11.

**Calculation procedure.**—The following procedure is used to determine the velocity and the thickness of the annular liquid film:

1. Determine the value of the flow-rate parameter  $\frac{W_i}{\pi D g \mu_o}$ .
2. Using this value, employ figure 11 to obtain the corresponding value of  $y^+$ .
3. The corresponding value of  $u^+$  is then obtained from figure 10.
4. The velocity or the thickness of the liquid film can then be determined from equation (B3) or equation (B5), respectively.

## DERIVATION OF FLOW-RATE PARAMETER

With the consideration of the continuity equation in the region near the wall where a velocity gradient is present



the flow rate per unit width  $w$  through the element  $dy$  is given by the relation

$$dw = g\mu u dy \quad (\text{B6})$$

Substituting the dimensionless parameters  $u^+$  and  $y^+$  from equations (B1) and (B4), respectively, in equation (B6) and assuming a constant density across the liquid film give the relation

$$\int_0^w dw = g\mu_0 \int_0^{y^+} u^+ dy^+$$

Thus

$$\frac{w}{g\mu_0} = \int_0^{y^+} u^+ dy^+ \quad (\text{B7})$$

The liquid flow per unit width  $w$ , can be approximated for a circular duct by dividing the total liquid flow  $W$ , by the circumference of the duct. The flow-rate parameter  $w^+$  for the liquid flow is thus obtained from equation (B7) as

$$w^+ = \frac{W}{\pi D g \mu_0} = \int_0^{y^+} u^+ dy^+ \quad (\text{B8})$$

The value of  $\int_0^{y^+} u^+ dy^+$  can be evaluated for any desired value of  $y^+$  by graphical integration of the curve of figure 10. The result of this graphical integration for various values of  $y^+$  is shown in figure 11.

## APPENDIX C

### EXAMPLE OF USE OF FIGURE 13(a) TO DETERMINE FILM-COOLANT REQUIREMENTS

In the following example, a determination is made of the coolant flow required to film cool a 4-inch-diameter tube with water supplied at 100° F for a distance of 1 foot with air flowing through the tube at 3 pounds per second and entering at 2000° F and with the pressure in the tube at 30 pounds per square inch absolute. Properties for air were obtained from references 15 and 16, and properties for water and water vapor were obtained from reference 19.

Because the average temperature  $T_{g,s}$  cannot be calculated without knowing the coolant flow, a first approximation of the coolant flow is made from figure 13(a) by calculating the ordinate of that figure with the air temperature at the entrance of the tube  $T_{g,1}$ , which in this case is 2000° F, in place of  $T_{g,s}$  and with the physical properties of air at that temperature. The ordinate  $Y$  of figure 13(a) is then calculated from the following:

$$L = 1.0 \text{ ft}$$

$$D = 1/3 \text{ ft}$$

$$k_s = 15.6 \times 10^{-6}$$

$$T_{g,1} - T_s = 2000 - 250 = 1750^\circ \text{ F}$$

$$\Delta H = C_{p,g}(T_s - T_i) + H_s = 1.0(250 - 100) + 945 = 1095 \text{ Btu/lb}$$

$$(Re)_s = \left( \frac{DG_s}{\mu_s} \right) = \left( \frac{34.4}{3 \times 34.5 \times 10^{-6}} \right) = 3.32 \times 10^5$$

$$Y = \frac{Lk_s(T_{g,1} - T_s)(Re)_s}{D(\Delta H)}$$

$$\frac{(1.0)(15.6 \times 10^{-6})(1750)(3.32 \times 10^5)}{(1/3)(1095)} = 24.9$$

From figure 13(a),  $W_g/\pi D = 0.072$  pound per second per foot and  $W_c = 0.072 \times \pi/3 = 0.075$  pound per second.

With the use of this coolant flow and the following equation,  $T_{g,2}$  is calculated.

$$W_g[C_{p,g}(T_{g,1} - T_{g,2})] = W_c[H_s + C_{p,s}(T_s - T_i) + C_{p,v}(T_{g,2} - T_s)]$$

Successive approximations are sometimes necessary because specific-heat values are averages for the temperature gradients. For the first approximation, the value for  $C_{p,g}$  is taken at  $T_{g,1}$  and the value for  $C_{p,s}$  is taken at an average between  $T_{g,1}$  and  $T_i$ :

$$3[0.283(2000 - T_{g,2})] = 0.075[945 + 1.0(250 - 100) + 0.52(T_{g,2} - 250)]$$

$$T_{g,2} = 1830^\circ \text{ F}$$

Further determinations will not appreciably affect the value of  $T_{g,2}$  in this case because the changes in specific heats are small. The calculation of  $T_{g,s}$  is then

$$T_{g,s} = \frac{2000 + 1830}{2} = 1915^\circ \text{ F}$$

The ordinate of figure 13(a) is then calculated with this value for average gas temperature  $T_{g,s}$  and with the physical properties of air at this temperature

$$Y = \frac{(1.0)(15.0 \times 10^{-6})(1915 - 250)(3.38 \times 10^5)}{(1/3)(1095)} = 23.1$$

From figure 13(a),  $W_g/\pi D = 0.066$  pound per second per foot and  $W_c = 0.066 \times \pi/3 = 0.069$  pound per second. Further calculations do not improve the determination appreciably; therefore a coolant flow of 0.069 pound per second is the requirement.

## REFERENCES

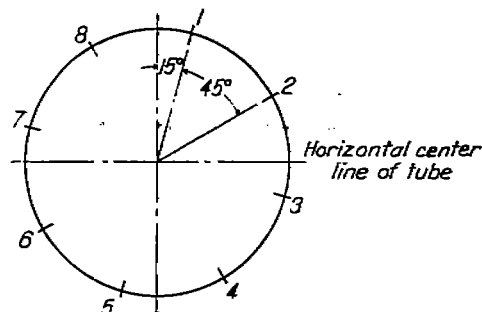
1. Dunn, Louis G., Powell, Walter B., and Seifert, Howard S.: Heat-Transfer Studies Relating to Rocket Power-Plant Development. Roy. Aero. Soc. and Inst. Aero. Sci., Third Anglo-American Aeronautical Conference (Brighton, England), Sept. 4-7, 1951, pp. 271-362.
2. Friedman, Joseph: A Theoretical and Experimental Investigation of Rocket-Motor Sweat Cooling. Jour. Am. Rocket Soc., no. 79, Dec. 1949, pp. 147-154.
3. Yuan, Shao Wen: Heat Transfer in Laminar Compressible Boundary Layer on a Porous Flat Plate with Fluid Injection. Jour. Aero. Sci., vol. 16, no. 12, Dec. 1949, pp. 741-748.
4. Lew, Henry G.: The Cooling of a Flat Plate in a Laminar Compressible Flow by Uniform Fluid Injection. PIBAL Rep. No. 131, Polytech. Inst. Brooklyn, Sept. 1, 1948. (Contract N6-ORI-206, Task Order 1, Proj. NR 061-001.)
5. Meyer-Hartwig, F.: Sweat Cooling of Nozzle Surfaces under High Thermal Stress. ATI 22204, Trans. No. F-TS-2067-RE, Wright-Patterson Air Force Base (Dayton, Ohio), Sept. 1948.
6. Eckert, E. R. G.: Heat Transfer and Temperature Profiles in Laminar Boundary Layers on a Sweat-Cooled Wall. Tech. Rep. No. 5646, Air Materiel Command, Nov. 3, 1947.
7. Kinney, George R., and Lidman, William G.: Investigation of Ceramic, Graphite, and Chrome-Plated Nozzles on Rocket Engine. NACA RM E8L16, 1949.
8. Sloop, J. L., and Kinney, George R.: Internal-Film Cooling of Rocket Nozzles. NACA RM E8A29a, 1948.
9. Boden, Robert H.: Heat Transfer in Rocket Motors and the Application of Film and Sweat Cooling. Trans. A.S.M.E., vol. 73, no. 4, May 1951, pp. 385-390.
10. Zucrow, M. J., Beighley, C. M., and Knuth, E.: Progress Report on the Stability of Liquid Films for Cooling Rocket Motors. Tech. Rep. No. 23, Purdue Univ., Nov. 30, 1950. (Contract N6-ORI-104, Task Order 1, NR 220-042, Phase 7, Project Squid.)
11. Gilliland, E. R., and Sherwood, T. K.: Diffusion of Vapors into Airstreams. Ind. and Eng. Chem., vol. 26, no. 5, 1934, pp. 516-523.
12. Ingebo, Robert D.: Vaporization Rates and Heat Transfer Coefficients for Pure Liquid Drops. NACA TN 2368, 1951.
13. Lockhardt, R. W., and Martinelli, R. C.: Proposed Correlation of Data for Isothermal Two-Phase, Two-Component Flow in Pipes. Chem. Eng. Prog., vol. 45, no. 1, Jan. 1949, pp. 39-45; discussion, pp. 45-48.
14. Bergelin, O. P.: Flow of Gas-Liquid Mixtures. Chem. Eng., vol. 56, no. 5, May 1949, pp. 104-106.
15. Ellenwood, Frank O., Kulik, Nicholas, and Gay, Norman R.: The Specific Heats of Certain Gases Over Wide Ranges of Pressures and Temperatures, Air, CO, CO<sub>2</sub>, CH<sub>4</sub>, C<sub>2</sub>, H<sub>4</sub>, H<sub>2</sub>, N<sub>2</sub>, and O<sub>2</sub>. Eng. Exp. Sta. Bull. No. 30, Cornell Univ., Oct. 1942.
16. Tribus, Myron, and Boelter, L. M. K.: An Investigation of Aircraft Heaters. II—Properties of Gases. NACA ARR, Oct. 1942.
17. von Kármán, Th.: The Analogy Between Fluid Friction and Heat Transfer. Trans. A.S.M.E., vol. 61, no. 8, Nov. 1939, pp. 705-710.
18. Deissler, Robert G.: Analytical and Experimental Investigation of Adiabatic Turbulent Flow in Smooth Tubes. NACA TN 2138, 1950.
19. Keenan, Joseph H., and Keyes, Fredrick G.: Thermodynamic Properties of Steam. John Wiley & Sons, Inc. (New York), 1936.
20. Anon.: Glycols. Carbide and Carbon Chemicals Corp., (New York, N. Y.), 1941.
21. McAdams, William H.: Heat Transmission. McGraw-Hill Book Co., Inc., 2nd ed., 1942.

TABLE I—PROPERTIES OF LIQUIDS FOR FLOW EXPERIMENTS \*

Liquid	Temperature (°F)	Absolute viscosity (lb-sec/sq ft)	Surface tension (dynes/cm)
Water	80	$1.84 \times 10^{-3}$	72
Water	210	.606	57
Water and 0.004-percent detergent	80	1.84	53
Water and 0.025-percent detergent	80	1.84	45
Water and 0.050-percent detergent	80	1.84	41
Water and 0.095-percent detergent	80	2.05	36
Water and 0.150-percent detergent	80	2.07	33
Water and 12-percent ethylene glycol	80	2.72	70
Water and 53-percent ethylene glycol	80	7.74	62
Water and 98-percent ethylene glycol	80	31.4	54

\* Water, reference 19; water and detergent, measured; water and glycol, reference 20.

TABLE II—LOCATION OF THERMOCOUPLES ON 4-INCH-DIAMETER FILM-COOLED TUBES

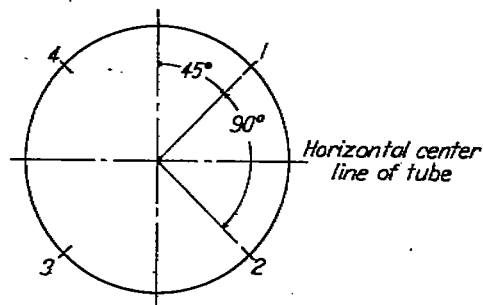


End view of tube in upstream direction showing circumferential positions of thermocouples

Circumferential position	Location of thermocouples—distance downstream of coolant injection (in.)	
	Rough-surface tube	Smooth-surface tube
1	2 to 25 <sup>a</sup> , 29, 33, 37, 41, 45	3 to 25 <sup>a</sup> , 29, 33, 37, 41, 45
2	13, 21, 29, 45	5, 9, 13, 17, 21, 25, 29, 45
3	2, 5, 9, 13, 21, 29, 45	5, 9, 13, 17, 21, 25, 29, 33, 37, 41, 45
4	13, 21, 29, 45	5, 9, 13, 17, 21, 25, 29, 45
5	2, 5, 9, 13, 21, 29, 45	5, 9, 13, 17, 21, 25, 29, 33, 37, 41, 45
6	13, 21, 29, 45	5, 9, 13, 17, 21, 25, 29, 45
7	2, 5, 9, 13, 21, 29, 45	5, 9, 13, 17, 21, 25, 29, 33, 37, 41, 45
8	13, 21, 29, 45	5, 9, 13, 17, 21, 25, 29, 45

\* Thermocouples located at 1-in. intervals in this range.

TABLE III—LOCATION OF THERMOCOUPLES ON 2-INCH-DIAMETER FILM-COOLED TUBE



End view of tube in downstream direction showing circumferential positions of thermocouple

Circumferential position	Location of thermocouples—distance downstream of coolant injection, in.
1	3, 5 to 42 <sup>a</sup>
2	5, 9 to 41 <sup>b</sup>
3	5, 9 to 41 <sup>b</sup>
4	5, 9 to 41 <sup>b</sup>

\* Thermocouples located at 1-in. intervals in this range.  
<sup>b</sup> Thermocouples located at 2-in. intervals in this range.

TABLE IV—EFFECT OF AIR-MASS VELOCITY, TUBE MATERIAL, AND TUBE DIAMETER ON LIQUID-FLOW TRANSITION REGION

[Liquid, water; air temperature, 80° F; Reynolds number,  $4.1 \times 10^4$  to  $28.6 \times 10^4$ ]

Air-mass velocity (lb/(sec)(sq ft))	Liquid-flow transition region <sup>a</sup> (lb/(sec)(ft))		
	Pyrex tube	Lucite tube	
	4 in.	4 in.	2 in.
30.6	0.032-0.063	0.035-0.065	0.037-0.060
44.5	.032-.068	.040-.068	.038-.063
70.0	.030-.068	.037-.073	.038-.062
108	.043-.068	.035-.070	.038-.062

\* From visual observations.

TABLE V—EFFECT OF LIQUID SURFACE TENSION ON LIQUID-FLOW TRANSITION REGION

[Pyrex tube diameter, 4 in.; air-mass velocity, 44.5 lb/(sec)(sq ft); air temperature, 80° F]

Liquid (percent by weight detergent in water)	Absolute viscosity at 80° F (lb-sec/sq ft)	Surface tension at 80° F (dynes/cm)	Liquid-flow transition region <sup>a</sup> (lb/(sec)(ft))
0.000	$1.84 \times 10^{-3}$	72	0.032-0.068
.004	1.84	65	.057-.062
.025	1.84	45	.063-.090
.050	1.84	41	.067-.090
.095	2.05	36	.068-.097
.150	2.07	33	Not determined

\* From visual observations.